International Journal of Scientific Research in Science and Technology
Available online at : www.ijsrst.com
Print ISSN: 2395-6011 | Online ISSN: 2395-602X
doi : https://doi.org/10.32628/IJSRST

An Investigation into the Solid-State Recycling of Aluminum Alloy AA2014 : A Mathematical Study

Rupesh Kumar Gupta, Dr Mahendra Yadav Suryakant
Department of Physics, Rama Bai Government women P. G. College, Akabarpur, Ambedkar Nagar Uttar Pradesh India

ARTICLEINFO

Article History:

Accepted: 07 Sep 2023
Published: 22 Sep 2023

Publication Issue
Volume 10, Issue 5
September-October-2023
Page Number
279-284

ABSTRACT

This research proposes mathematical models that link the process parameters used in direct recycling of aluminium alloy AA2014 to the mechanical qualities of the resulting semi products. Without any further processing, the desired mechanical qualities can be obtained from extruded materials alone. The primary goal of the research was to evaluate and contrast several simulations and mathematical models of aluminium chip solid-state recycling. The study's overarching goal is to assess how well they predict important recycling-related variables and outcomes.

Keywords: AA2014, Compacting force, extrusion temperature, yield strength, percent elongation, ultimate tensile strength

I. INTRODUCTION

One way to better understand and optimise the SSR process for aluminium chips is to conduct a comparative assessment of the mathematical models and analyses currently in use. Aluminium chips are a byproduct of many manufacturing processes; recycling them by SSR is both cost-effective and environmentally friendly. The goal of a comparative study of mathematical analyses in solid state recycling of aluminium chips should be to shed light on the efficacy and efficiency of the process, allowing for better decisions to be made by researchers and practitioners towards the goal of sustainable aluminium chip recycling. It should also draw attention to the need for improved research and modelling in specific areas. The purpose of this comparison is to shed light on the relative merits of several mathematical models or simulations employed in the solid-state recycling of aluminium chips. This data will help scientists and engineers pick the best models for their projects and make recycling more efficient.

Microhardness of AA6061 chip and powder blends produced by cold forging was studied by Kadir et al. in 2017. When compared to the original material, the mixture containing 78.5% powder of size 25 m and 21.5% powder of size 100 m showed 25% lower microhardness.

The mechanical characteristics and microstructure of solid-state recycled AA6061 chips were investigated by Abd El Aal et al. (2018), who looked at the impact of extrusion temperature and extrusion ratio. Using the Box-Behnken design (BBD) method, Lela et al. (2016) prepared experiments to solid-state recycle AW2011 chips. Solid-state recycling, as described by Koch et al. (2021), necessitates roughly 3.2 GJ/ton with nearly no material losses. Solid-state recycling of AA7075 chips reinforced by zirconium dioxide (ZrO2) nanoparticles via direct extrusion and ECAP, then heat treatment, was achieved by Sabbar et al. (2021). An environmentally acceptable method of recycling the aluminium alloy AA2011 was presented by Wagdy et al. (2022). The turning operation's byproduct chips were gathered, pressed into billets, and hot extruded. Two steps, direct rolling and accumulative roll bonding, make up the innovative solid-state recycling method for aluminium chips, which Mehtedi et al. (2023) described in detail as a life cycle assessment (LCA) examination of the environmental benefits of this process.

2. Design of experiments: The purpose of this research is to develop mathematical models that explain the connection between the mechanical properties of an extrudate and the chip size, the cold compacting force, and the extrusion temperature. Design of experiments (DOE) and correlation regression analysis (RA) are two methods that can be used to obtain such models. Selecting a range of investigated process parameters is the first stage in well-planned experiments, and here, both prior knowledge and first-hand experience came in handy. The process parameters that were determined to be varied were the depth of cut from (0.6 to 1.78 mm), the compaction force (200 to 510 kN), and the extrusion temperature (310 to 520 °C). In order to implement the DOE, a Box-Behnken (BBD) response surface design was employed. Since BBD allows for optimisation and can reduce the number of experiments needed, it is widely utilised in experimental research and modelling. There must be a total of 17 tests, including 12 for the three-factor BBD (one for each level of the factor) and five for the central factor.

II. MATERIAL AND METHODS

Turning a bar of 701000 mm with an Iskar tool that consists of a tool holder and a cutting insert, chips of EN AW 2014 were created. If the cutting depth, feed rate, and cutting edge angle of the tool are known, then the cross-sectional area may be easily determined. The tool with which this study was conducted has a cutting edge angle of 95 degrees. Turning with depth of cut produced spiral-shaped chips with an average length of 5 mm and a cross-sectional area of 0.0805 mm2. Chips with an average length of 30 mm and cross-sectional area of 0.15 mm2 were produced by turning with a depth of cut of 1.150 mm. When the aluminium bar was twisted with a 1.78 mm depth of cut, the chips formed a continuous spiral. The typical dimensions of these chips were 215 mm in length and 0.25 mm 2 in cross-sectional area. As the collected chips were all in the shape of a cylindrical coil (or helix), the total developed length and, by extension, volume, may be calculated. The number of turns, combined height, and width of chips must be determined. Using the required dimensions, the average volumes of chips created from turning with cut depths of 0.5, 1.150, and 1.78 mm were determined to be 1.38, 29 mm3, and 178 mm3, respectively. It is clear that chips vary widely in geometry and dimensions; this variety will be useful in determining how chip geometry affects the solid-state recycling process.

The initial, cold compacting phase was carried out using a 1.1 MN hydraulic press. According to the experimental design, 17 billets were produced by compacting chips with 210, 360, and 550 kN. A 35 mm inner diameter die and a 35 mm inner diameter punch were used to accomplish the compacting. The compacting procedure resulted in a significant reduction in volume and required several steps before it was accomplished. First, volume was created via compaction; next, additional chips were added and compacted, and so on, until a final length of at least 55 mm was reached. HBM's C6A 1MN load cell and WAT's inductive displacement sensor were used to determine the compacting force and punch displacement, respectively. The speed of the punch was 1.1 mm/s. The force required to remove billets from the die after compacting them ranged from 55 to 110 kN.

Using the same hydraulic press employed in the compacting process, hot extrusion was performed. The extrusion container had a 42 mm diameter. The crushed billets were then fed into a flat die with an aperture diameter of 17 mm to create solid sections. We were able to attain a 7.1:1 extrusion ratio. Extrusion container and die were heated to 325, 430, or 540 °C for each billet, as per the experimental design. Omron's temperature regulator and relay were used to maintain a steady temperature. For 30 minutes before to extrusion, each billet was warmed in the furnace at the appropriate extrusion temperature. The velocity of the punch was 1 mm/s. The surface quality of all the acquired pieces was quite acceptable, with the exception of a few that had minor flaws such as blistering or cracking. In Figure 5, we see a solid portion (and the die) extruded from billet no. 1. Lack of considerable plastic deformation at the beginning of the segment is clearly visible as a major difference in quality between the beginning and the rest of the section.

III. RESULTS AND DISCUSSION

The Instrone 8801 universal testing equipment was used to calculate the material's ultimate tensile strength (R_m), yield strength$R_p(0.2)$, and percent elongation (PE). The resulting pieces were then used to turn out standard tensile specimens (gauge diameter: 5.5 mm). Using the offset method, in which a line is drawn perpendicular to the linear stress-strain segment of the curve and crosses at the 0.003 point on the strain axis, the yield strength was calculated. The point where this line and the stress-strain curve meet is when the yield strength (offset by 0.25% from its true value) is determined.

Engineering strain, tensile strength, and yield strength for recycled samples fall between 4.3 and 9.6% and 192.4 to 240 MPa, respectively. Mathematical models for *Rm*, *Rp0.2*, and *PE.* were derived after the data was entered into the computer programme Design- Expert and RA were run on the data. Both depth of cut and compaction force were found to be unimportant model factors in the linear mathematical model proposed for *Rm*, as determined by analysis of variance. Values of 0.71 for R-Squared, 0.64 for Adjusted R-Squared, and 0.49 for Precision were found. Cut depth, extrusion temperature, and compaction force will hereafter be denoted by the letters A, B, and C, respectively.

The extrudates' microstructural homogeneity was evaluated using optical microscopy on their cross section. Each extrudate was sliced into 22 mm tall cylindrical pieces. The samples were cut in half, ground, polished, and etched before being examined under a 90x optical microscope. Micrographs obtained showed that certain extruded parts had a microstructure with inhomogeneities and fractures.

All 300 °C extruded samples broke, with a trend towards smaller breaks as chip size decreased. On the other hand, raising the extrusion temperature reduces the severity of cracks and improves the uniformity of the microstructure.

B: extrusion temperature (°C) x	C: compaction force (kN) y	Ultimate tensile strength (MPa) z
300	350	194.2
300	200	215.2
400	500	219.7
500	350	247.8
400	500	214.6
300	500	201
400	350	207
400	350	215.4
400	350	217.8
400	200	211.9
500	350	232
300	350	197.5
500	200	243.2
400	350	207.9
500	500	222.8
400	200	210.8
400	350	217.2

$$z = 234.6424 - 0.2329\,x - 0.0367y + 0.0006x^2 - 0.0001xy + 0.0001y^2$$
$$r^2 = 0.7869, {r^2}_{adj} = 0.69$$

Graph 1: 3D surface plot of Ultimate tensile strength (MPa) for extrusion temperature (°C) and compaction force (kN)

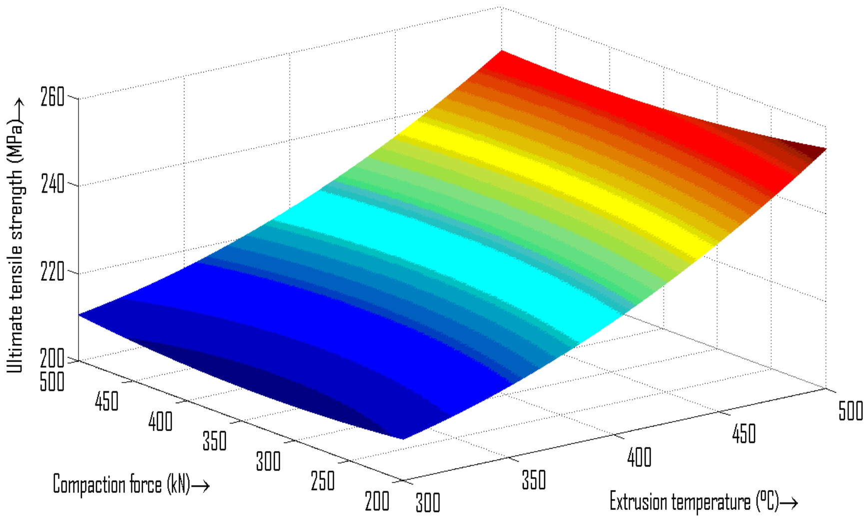

A: depth of cut (mm) x	B: extrusion temperature (°C) y	Yield strength (MPa) z
0.4	300	97.98
1.025	300	119.98
1.65	400	111.98
0.4	500	106.98
0.4	400	104.98
1.025	300	124.98
1.025	400	88.98
1.025	400	90.98
1.025	400	94.98
0.4	400	93.98
1.65	500	97.98
1.65	300	136.98
1.025	500	109.98
1.025	400	78.98
1.025	500	102.98
1.65	400	106.98
1.025	400	89.98

$$z = 309.6594 + 54.6215\,x - 1.1712y + 15.6968x^2 - 0.192xy + 0.0016y^2$$

$$r^2 = 0.7943, r^2{}_{adj} = 0.7008$$

Graph 2: 3D surface plot of yield strength (MPa) for depth of cut (mm) and extrusion temperature (°C)

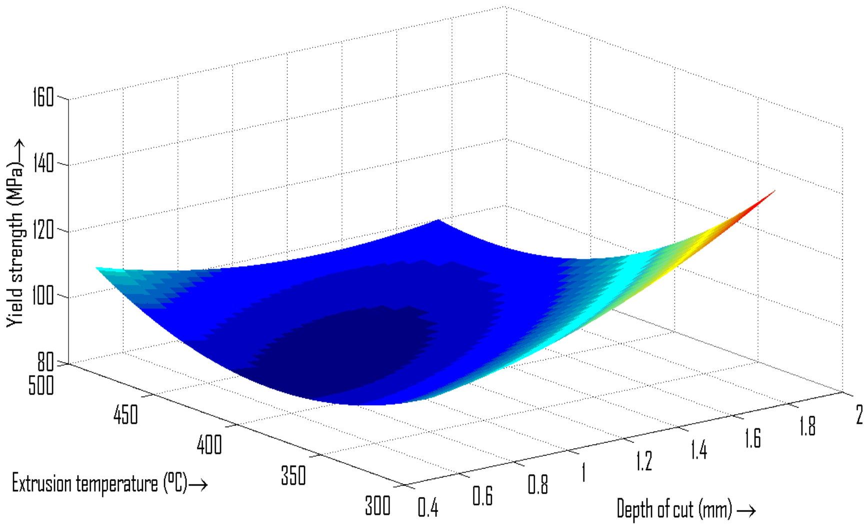

B: extrusion temperature (°C) x	C: compaction force (kN) y	Percent elongation (%) z
300	350	10.08
300	200	8.98
400	500	7.18
500	350	5.08
400	500	9.38
300	500	8.18
400	350	7.48
400	350	7.98
400	350	8.48
400	200	9.18
500	350	4.68
300	350	10.58
500	200	5.58
400	350	8.38
500	500	4.78
400	200	9.38
400	350	8.08

$$z = 0.0161 + 0.0699x - 0.0038y - 0.0001x^2$$
$$r^2 = 0.8604, r^2{}_{adj} = 0.7969$$

Graph 3: 3D surface plot of percent elongation (%) for extrusion temperature (°C) and compaction force (kN

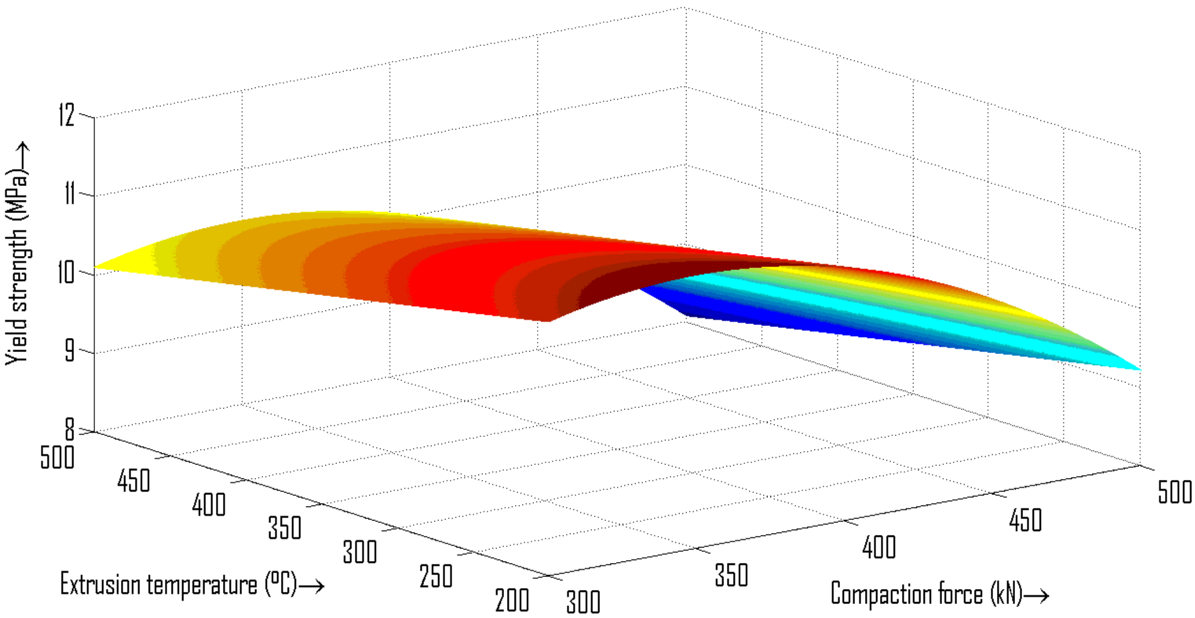

IV. CONCLUSION

The ultimate tensile strength is not affected by the compaction force or the size of the chip, but rather by the extrusion temperature. The maximum tensile strength grows in tandem with the temperature. When the extrusion temperature was 450 degrees Celsius, the compaction force was 190 kN, and the depth of cut was 0.6 mm, R_m=237.8 MPa was achieved.

Yield strength is affected by chip size and temperature, but not by the amount of force used to compact the material. If the compaction force is held constant and the chip size is maximised, then lowering the extrusion temperature will increase the yield strength. When the extrusion temperature is between 250 and 350 °C and the depth of cut is increased, the yield strength likewise increases, but it decreases when the extrusion temperature is between 450 and 550 °C and the depth of cut is increased. When the extrusion temperature is 325 °C, the depth of cut is 1.70 mm, and the compaction force is 410 kN, the maximum R_p (0.15)=135 MPa is reached.

However, compaction force and extrusion temperature do affect % elongation, but chip size does not. Extrusion temperature has a negative effect on percent elongation for a given chip size. The percentage of elongation increases very marginally as the compaction force decreases. With a 0.6 mm depth of cut, 350 °C extrusion temperature, and 225 kN compaction force, the maximum percent elongation is 10%.

Cross-sectional optical microscopy analysis of the extrudates reveals that those formed from the biggest chips and extruded at 350 °C had poor metallic bonding between chips, as evidenced by the prevalence of cracks and inhomogeneities. All of the 350 °C extruded samples developed cracks, albeit the severity of the cracks decreased along with the chip size. The best microstructure came from using the highest extrusion temperature and the tiniest chips. Unfortunately, the connection between crack size and compaction force was missed.

To get the highest possible mechanical property values, the optimal process parameters are cut depth, extrusion temperature, and compaction force. The values of 1.71 mm, 360 °C, and 210 kN were found to correspond to the values of R_p (0.15)=118.3 MPa, R_m=211.4 MPa and PE=9.3 % , respectively. The settings give the best possible mechanical qualities, yet this semiproduct has flaws in the microstructure, rendering it useless.

Since the aluminium alloy employed in the study can be heat treated, future studies should investigate the effect of heat treatment on extrudate characteristics. Another study should be conducted with a higher extrusion temperature and ratio to eliminate microstructure cracks.

V. REFERENCES

[1]. Abd El Aal, M. I., Taha, M. A., Selmy, A. I., El-Gohry, A. M., and Kim, H. S. (2018). Solid state recycling of aluminium AA6061 alloy chips by hot extrusion. Materials Research Express, 6(3).

[2]. Kadir, M. I., Mustapa, M. S., Mahdi, A. S., Kuddus, S., andamp; Samsi, M. A. (2017). Evaluation of hardness strength and microstructures of recycled al chip and powder AA6061 fabricated by cold compaction method. IOP Conference Series: Materials Science and Engineering, 165.

[3]. Koch, A., Henkel, T., and Walther, F. (2021). Mechanism-oriented characterization of the anisotropy of extruded profiles based on solid-state recycled EN AW-6060 aluminum chips. Engineering Failure Analysis, 121.

[4]. Lela, B., Krolo, J., and Jozić, S. (2016). Mathematical modeling of solid-state recycling of aluminum chips. The International Journal of Advanced Manufacturing Technology, 87(1-4), 1125-1133.

[5]. Mehtedi MEI, Buonadonna P., Carta M. , Mohtadi REI, Mele A., Morea D. (2023): “Sustainability study of a new solid-state aluminum chips recycling process: a life cycle assessment approach”, Sustainability, 15:1-14.

[6]. Sabbar, H. M., Leman, Z., Shamsudin, S., Tahir, S. M., Jaafar, C. N., Ariff, A. H., Zahari, N. I.,andRady, M. H. (2021). The Effect of Solid-State Processes and Heat Treatment on the Properties of AA7075 Aluminum Waste Recycling Nanocomposite. Materials, 14(21), 6667.

[7]. Wagdy B., Ayman A., El-Wahab A., El-gamasy R. (2022): “Statistical analysis of solid-state recycled aluminum alloy 2011 chips by hot extrusion”, Engineering Science and Military Technologies, 6(2):86-94.

Cite this article as :

Rupesh Kumar Gupta, Dr Mahendra Yadav Suryakant, "An Investigation into the Solid-State Recycling of Aluminum Alloy AA2014 : A Mathematical Study ", International Journal of Scientific Research in Science and Technology (IJSRST), Online ISSN : 2395-602X, Print ISSN : 2395-6011, Volume 10 Issue 5, pp. 279-284, September-October 2023.

Journal URL : https://ijsrst.com/IJSRST52310521